Chinese Journal of Chemistry, **2004**, *22*, 611—615 **Article**

Quantum Chemical Study on the Reaction Mechanism of OBrO Radical with OH Radical

ZHAO, Min[a,b](赵岷) ZHAO, Yan-Ling[a](赵艳玲) LIU, Peng-Jun[a](刘朋军)
CHANG, Ying-Fei[a](常鹰飞) PAN, Xiu-Mei[a](潘秀梅) SU, Zhong-Min[a](苏忠民)
WANG, Rong-Shun*[,a](王荣顺)

[a] *Institute of Functional Material Chemistry, Faculty of Chemistry, Northeast Normal University, Changchun, Jilin 130024, China*
[b] *School of Science of Chemistry and Food, Bohai University, Jinzhou, Liaoning 121000, China*

The reaction mechanism of OBrO with OH has been studied using the B3LYP/6-311+G(d,p) and the high-level electron-correlation CCSD(T)/6-311+G(d,p) at single-point. The results show that the title reaction could probably proceed by four possible schemes, generating $HOBr+O_2$, $HBr+O_3$, $BrO+HO_2$ and $HOBrO_2$ products, respectively. The main channel is the one to yield $HOBr+O_2$. The whole reaction involves the formation of three-membered, four-membered and five-membered rings, followed by the complicated processes of association, H-shift, Br-shift and dissociation. All routes are exothermic.

Keywords OBrO, OH, reaction mechanism, transition state

Introduction

Since it is realized that the halogen oxides in atmosphere destroy the ozone layer contained in stratosphere, both experimental and theoretical scientists have paid much attention to the investigation of the possibly occurring chemical reactions there.[1] It is known that the halogen oxide species, mainly including ClO, BrO, OClO and OBrO, which exist in polar stratospheres,[2-4] will produce halogen atoms by the photodissociation. Resulting from the reaction of halogen atoms with O_3, the ozone layer is damaged to some extent. As one of halogen-containing oxide radicals, OBrO could be experimentally produced in a discharge flow reactor by using three methods: (1) $O+Br_2$, (2) $Br+O_3$ and (3) microwave discharge of a Br_2/O_2/He mixture. In addition, there have been some correlative research reports about the reactions of OBrO with other atmospheric species.[5-7]

In spite of the low content in atmosphere, OH radical plays an important role in the atmospheric photochemistry for its lively reactivity. So far, there has been a preliminary study experimentally on the reaction of OClO radical with OH radical[8,9] by proposing two possible schemes to generate $HOCl+O_2$ and $ClO+HO_2$ products, respectively. Theoretically, Xu *et al.*[10] and our group[11] have investigated the kinetics and mechanism of $OClO+OH$ by *ab initio* and DFT methods, respectively. However, there is not yet report about the reaction of OBrO with OH. Due to the similar electronic structure of OBrO to that of OClO, it is supposed that they ought to possess analogous reactive characteristics.

The calculation methods of quantum chemistry are always thought of an important way to investigate the microcosmic mechanism of instant reactions.[12] In this paper, the reaction mechanism of OBrO with OH is theoretically studied using the B3LYP/6-311+G(d,p) and the high-level electron-correlation CCSD(T)/6-311+G(d,p) at single-point. The theoretical results are meaningful and helpful to fully understand the atmospheric chemistry of OBrO.

Calculation details

The geometrical structures of all reactants, intermediates, transition states and products for the possible chemical reactions of OBrO with OH were fully optimized by means of Schlegel's algorithm[13] using density functional theory. Afterwards, the harmonic frequency calculations were performed to verify whether each of them has its own right critical index and simultaneously to obtain the corresponding zero-point energy correction. Moreover, to get more reliable total energies of each system, the structures determined on the level of B3LYP/6-311+G(d,p) were used to calculate the single-point energy at the high level of CCSD(T)/6-311+G(d,p) (denoted as CCSD(T)/6-311+G(d,p)//B3LYP/6-311+G(d,p)). To confirm that the transition-state structure is the saddle point connecting the correspond-

* E-mail: wangrs@nenu.edu.cn
Received July 7, 2003; revised January 5, 2004; accepted February 28, 2004.
Project supported by Ministry of Education (the training project of elitist) Foundation ([2001] 3) and the Young Teacher Fund of Northeast Normal University (No. 111382).

ing reactants and products of interest, Intrinsic Reaction Coordinate (IRC) calculations were further performed. All calculations were carried out with the Gaussian 98 program package.

Results and discussion

Analysis of the geometries and frequencies of all stationary points in reaction paths

The structure parameters of the reactants, products, intermediates (IM) and transition states (TS) are illustrated in Figure 1. And the energies of various structure on the level of B3LYP and CCSD(T) are respectively listed in Table 1, by regarding the energy of reactants as zero for comparison. Furthermore, on the level of CCSD(T) theory, the energy variations of the reaction routes for OBrO and OH are clearly depicted in Figure 2.

As shown in Figure 1 and Figure 2, for the reaction of OBrO with OH, there are totally four IM, nine TS and four products on the potential energy profile. From the picture, it is found that these four IM and product $HOBrO_2$ are five thermodynamically stable isomers, among which IM1 may be easily isomerized into IM2 due to the low energy barrier (from IM1 to TS1, ΔE= 9.35 kJ • mol^{-1}) and vice versa (from IM2 to TS1, ΔE= 17.38 kJ • mol^{-1}), so do IM3 and IM4. However, the isomerization of $HOBrO_2$ seems difficult for its high activation energy (from $HOBrO_2$ to TS5, ΔE=135.19 kJ • mol^{-1}). Thus, different from other isomers (IM1—IM4), only the product of $HOBrO_2$ is kinetically the most stable.

In order to verify IM and TS, the harmonic frequency calculations are performed for all stationary points. Since these systems all include five atoms, they should have nine vibrational modes according to the formula of $3N-6$ (N stands for the atom number of the system). It is well known that transition state has only one vibrational mode with an imaginary frequency. The imaginary frequencies of nine TS are listed as follows: 345.74i cm^{-1} (TS1), 152.16i cm^{-1} (TS2), 207.84i cm^{-1} (TS3), 1183.19i cm^{-1} (TS4), 398.98i cm^{-1} (TS5), 327.43i cm^{-1} (TS6), 148.00i cm^{-1} (TS7), 116.62i cm^{-1} (TS8), 1745.39i cm^{-1} (TS9), respectively. The vibrational modes pictured in Figure 3 clearly reveal the vibrational directions and chemical properties of all TS structures. As for the intermediates, they are confirmed to be local minima with the positive frequencies on the

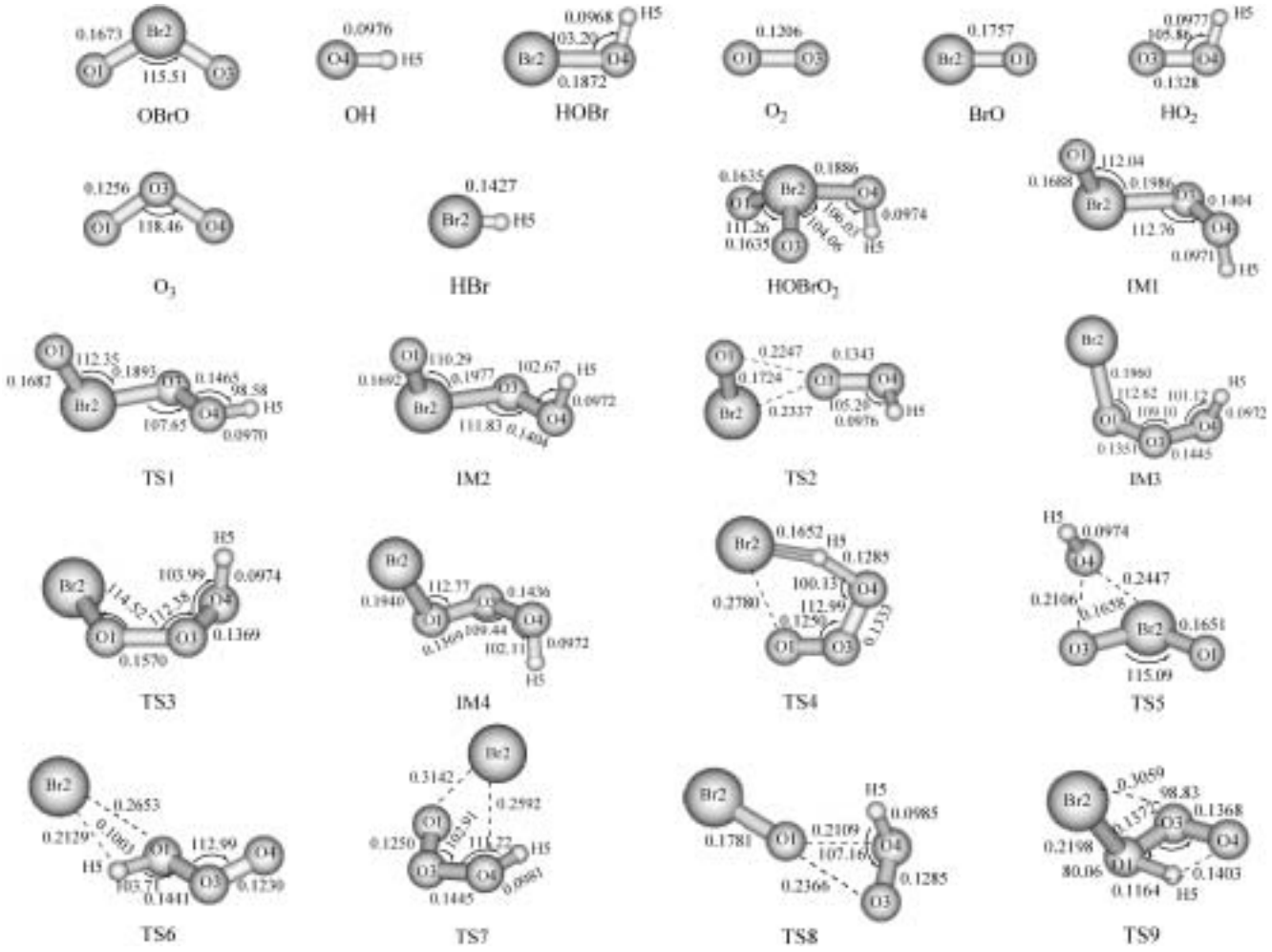

Figure 1 Optimized geometries of various species calculated at the B3LYP/6-311+G(d,p) level (bond lengths are given in nm and bond angles in degrees).

Table 1 Zero-point correction energies (E_{ZPC}), total energies (E_T) and relative energies (ΔE) of all species calculated at the B3LYP/6-311+G(d,p) and single-point CCSD(T)/6-311+G(d,p) levels

Species	B3LYP			CCSD(T)	
	E_{ZPC}/a.u.	E_T/a.u.	ΔE/(kJ · mol^{-1})	E_T/a.u.	ΔE/(kJ · mol^{-1})
OBrO+OH	0.01276	−2800.18385	0.0	−2798.04328	0.0
IM1	0.01874	−2800.21264	−75.59	−2798.07175	−74.75
TS1	0.01798	−2800.20797	−63.33	−2798.06819	−65.40
IM2	0.01887	−2800.21574	−83.73	−2798.07481	−82.78
TS2	0.01877	−2800.19023	−16.75	−2798.06372	−53.67
IM3	0.01947	−2800.24496	−160.44	−2798.10774	−169.24
TS3	0.01937	−2800.22796	−115.81	−2798.09141	−126.37
TS4	0.01357	−2800.20610	−58.42	−2798.06957	−69.02
TS5	0.01660	−2800.15771	68.63	−2798.02865	38.41
IM4	0.01958	−2800.24525	−161.21	−2798.10813	−170.26
TS6	0.01733	−2800.19187	−21.06	−2798.09285	−130.15
TS7	0.01858	−2800.19299	−24.00	−2798.07598	−85.85
TS8	0.01802	−2800.18585	−5.25	−2798.06839	−65.93
TS9	0.01527	−2800.17158	32.21	−2798.03865	12.16
$HOBrO_2$	0.01836	−2800.22219	−100.66	−2798.08014	−96.78
$BrO+HO_2$	0.01564	−2800.22373	−104.70	−2798.08139	−100.06
$HBr+O_3$	0.01315	−2800.22050	−96.22	−2798.09654	−139.83
$HOBr+O_2$	0.01632	−2800.23631	−137.73	−2798.11457	−187.17

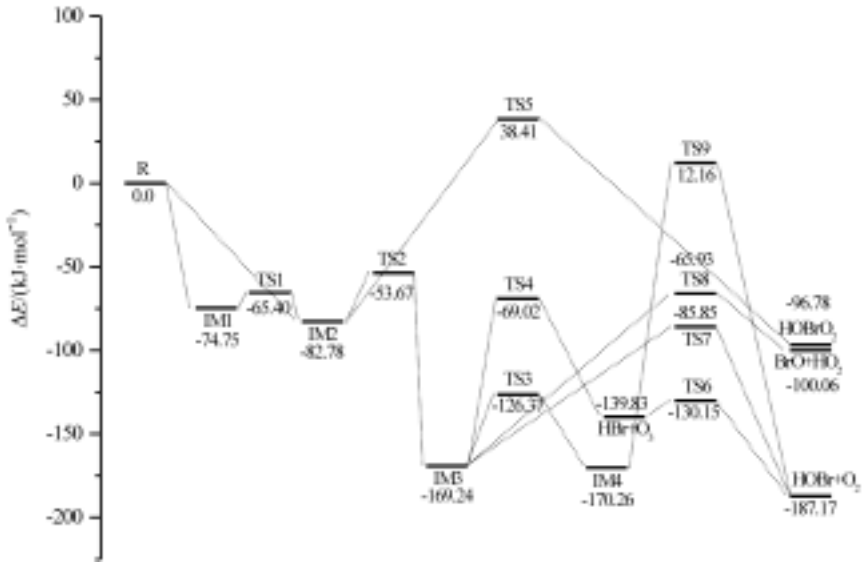

Figure 2 The energy variation of the reaction route of OBrO and OH.

potential energy profile. On the other hand, Intrinsic Reaction Coordinate (IRC) calculations, which testify that the transition states connect the right reactants, intermediates and products, could also give the same evidence to distinguish every structure characteristics.

Analysis of the reaction mechanism

The reaction of OBrO with OH is a kind of double radical reaction. As OBrO radical approaches OH radical, the p-electrons from O atoms on both OBrO and OH will quickly form a bond, leaving behind non-plane and chain-like intermediates, IM1 and IM2 respectively. These two processes are both barrier-free, with exothermic energy of 74.75 and 82.78 kJ · mol^{-1}, respectively. Moreover, the low energy IM1 and IM2 are energetically closer so that they could easily convert to

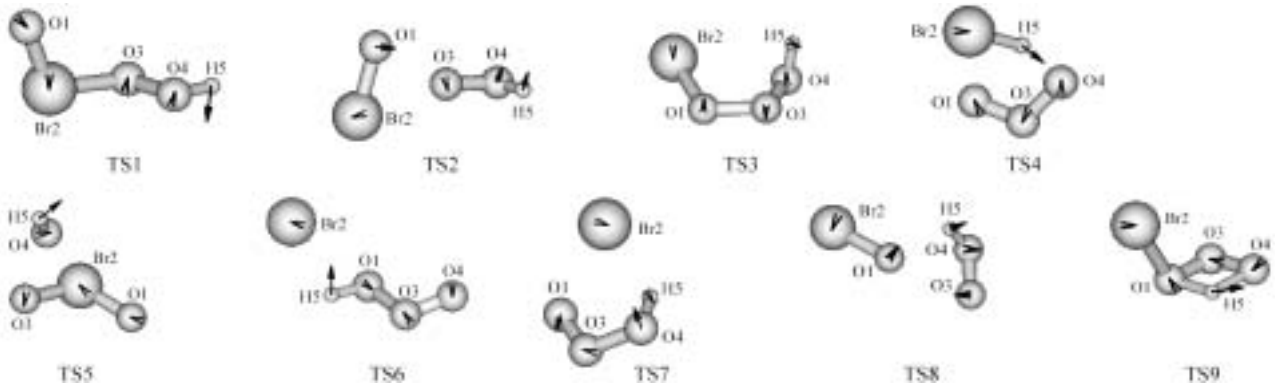

Figure 3 Imaginary vibrational modes of transition states

each other through TS1. Afterwards, IM2 goes on further change along four different channels, generating four different products. Associated with Figure 1 and Figure 2, these four schemes will be discussed in the following, respectively.

Scheme 1 The products are HBr and O_3. Through low energy barrier (IM2→TS2, $\Delta E=29.11$ kJ · mol^{-1}), IM2 converts into IM3. The whole process undergoes the formation and breakage of a three-membered ring of O(1)Br(2)O(3), followed by the rotation of O(4)—H(5) single bond. Then, through TS4 (IM3→TS4, $\Delta E=100.22$ kJ · mol^{-1}), which shows a five-membered ring of O(1)O(3)O(4)H(5)Br(2), the H(5) attached to O(4) from IM3 is gradually linked with Br(2), leading to the broken bond of O(4)—H(5). Simultaneously, the distance between Br(2) and O(1) is continuously enlarged so as to finally yield the products of HBr and O_3. Owing to the high barrier, the transformation of IM3→TS4 is the rate-controlling step for channel 1.

Scheme 2 The products are HOBr+O_2. Different from channel 1, channel 2 respectively begins with IM3 and products of HBr+O_3, undergoes different pathways, but finally achieves the same products of HOBr+O_2. Starting from IM3, there are two different pathways. The first one gets across an energy barrier of 83.39 kJ · mol^{-1} (IM3→TS7) and reaches the destination (products of HOBr+O_2), with the increase of O(1)—Br(2) bond length and the decrease of Br(2)—O(4) bond length. In fact, this process is also regarded as the Br-shift between O(1) and O(4), followed by the rupture of O(3)—O(4) bond, and sequentially achieves products of HOBr+O_2. As for the second one, IM3 is easily isomerized into IM4 by TS3 (IM3→TS3, $\Delta E=$ 42.87 kJ · mol^{-1}). Afterwards, IM4 gets to products of HOBr+O_2 by TS9, which involves the formation of a four-membered ring of O(4)O(3)O(1)H(5), with an activation energy of 182.42 kJ · mol^{-1} (IM4→TS9). The H(5)-shift from O(4) to O(1) and the breakage of O(1)—O(3) bond result in the desired products of HOBr+O_2. On the other hand, beginning with products of HBr+O_3, the pathway smoothly goes through TS6 (HBr+O_3→TS6, $\Delta E=9.68$ kJ · mol^{-1}), accomplishing the conversion from HBr+O_3 to HOBr+O_2. Eventually, by comparing energy barriers of the three pathways in channel 2, it is found that the route through TS7 is the most favorable. Therefore, the rate-controlling step of IM3→TS7 could be known.

Scheme 3 The products are BrO+HO_2. In comparison with channel 1, this channel goes along different path beginning with IM3. From IM3 to TS8, the energy barrier is 103.31 kJ · mol^{-1}. In TS8, the distance between O(1) and O(3) is 0.2366 nm, indicating that the bond is broken. Moreover, IRC calculation shows that this distance is further increased, ultimately resulting in products of BrO+HO_2.

Scheme 4 In particular, the product of $HOBrO_2$ is an addition product. By comparison with channel 1, this channel presents different route starting from IM2. With the energy barrier of 121.19 kJ · mol^{-1} (IM2→TS5), IM2 is distorted into a transitional three-membered ring of Br(2)O(3)O(4). Later, the Br(2)—O(4) bond is gradually formed, followed by the breakage of O(3)—O(4) bond so as to produce the addition product of $HOBrO_2$. Rather, the possibility for this channel to go on is small due to the high activation energy.

Energy variation of the reaction route of OBrO with OH

Figure 2 describes the relative energy variations of all stationary points, by taking the reactant energy as zero for comparison. In this picture, we could find that the pathway, R→IM2→TS2→IM3→TS7→HOBr+O_2, is the best reaction one in channel 2 attributed to its low energy barriers (IM3→TS7, $\Delta E=83.39$ kJ · mol^{-1}), fast reaction rate and the stable products (for HOBr+O_2, its relative energy is the lowest among all products). Rather, the reactions along channel 1, R→IM2→TS2→IM3→TS4→HBr+O_3, and channel 3, R→IM2→TS2→IM3→TS8→BrO+HO_2, proceed with nearly equal rate due to their close energy barriers of 100.22 kJ · mol^{-1} (IM3→TS4) and 103.31 kJ ·mol^{-1} (IM3→TS8), respectively. As for channel 4, R→IM2→TS5→$HOBrO_2$, it kinetically passes through slowly for the high energy barrier (IM2→TS5, $\Delta E=121.19$ kJ · mol^{-1}). Relative to the reactant energy, the energies of products HOBr+O_2, HBr+O_3, BrO+HO_2 and $HOBrO_2$ are −187.17, −139.83, −100.06 and −96.78 kJ · mol^{-1}, respec-

tively, which clearly show that the channels are all exothermic.

Conclusions

The reaction of OBrO with OH is an exothermic process by multi-channel and multi-steps. Four products, $HOBr+O_2$, $HBr+O_3$, $BrO+HO_2$ and $HOBrO_2$, could be obtained. According to the kinetic and thermodynamic calculation results, it proves that the main product is $HOBr+O_2$. The whole reaction mechanism involves the formation of three-membered, four-membered and five-membered rings, followed by the complicated processes of association, H-shift and dissociation.

By contrast with the previous studies of OClO+OH,[11] it is found that the two reactions (OClO+OH, OBrO+OH) both undergo four product channels and have analogous reaction mechanism. Furthermore, comparing the activation energies of their optimal reaction routes, we could conclude that the rate of OBrO+OH is faster than that of OClO+OH under the same reaction conditions.

Theoretically, we investigate the mechanism of the reaction of OBrO with OH. All the results need to be further testified by experiment.

References

1 Wang, Z. Y.; Li, H. Y.; Zhou, S. K. *Chin. Sci. Bull.* **2001**, *46*, 619 (in Chinese).
2 Solomon, S. *Nature* **1990**, *347*, 347.
3 Renard, J. B.; Pirre, M.; Robert, C.; Huguenin, D. *J. Geophys. Res.* **1998**, *103*, 25383.
4 Sanders, R. W.; Solomon, S.; Kreher, K.; Johnston, P. V. *J. Atmos. Chem.* **1999**, *33*, 283.
5 Li, Z. *J. Phys. Chem. A* **1999**, *103*, 1206.
6 Li, Z.; Tao, Z. *Chem. Phys. Lett.* **1999**, *306*, 117.
7 Li, Z.; Jeong, G. R.; Person, E. *Int. J. Chem. Kinet.* **2002**, *34*, 430.
8 Poulet, G.; Zagogianni, H.; LeBras, G. *Int. J. Chem. Kinet.* **1986**, *18*, 847.
9 Grela, M. A.; Colussi, A. J. *J. Phys. Chem.* **1996**, *100*, 10150.
10 Xu, Z. F.; Zhu, R.; Lin, M. C. *J. Phys. Chem. A* **2003**, *107*, 1040.
11 Zhao, M.; Pan, X. M.; Liu, P. J.; Sun, H.; Su, Z. M.; Wang, R. S. *Acta Chim. Sinica* **2003**, *61*, 1192 (in Chinese).
12 Liu, P. J.; Pan, X. M.; Zhao, M.; Sun, H.; Su, Z. M.; Wang, R. S. *Acta Chim. Sinica* **2002**, *60*, 457 (in Chinese).
13 Schlegel, H. B. *J. Comput. Chem.* **1982**, *3*, 21.

(E0307076 PAN, B. F.)